Modeling Bubble Growth and Departure from a Cavity

Mehran Mohammadi Farhangi[1] and Mohammad Passandideh-Fard[2]

[1]Graduate Student, [2]Assistant Professor (mpfard@um.ac.ir)
Department of Mechanical Engineering, Ferdowsi University of Mashhad, Mashhad, Iran

ABSTRACT

In this paper, the characteristics of bubble growth and departure of a bubble from a cavity is simulated using a transient 2D/axisymmetric model. To predict the shape of the bubble deformation, the Navier-Stokes equations in addition to an advection equation for liquid volume fraction are solved. A modified Volume-of-Fluid (VOF) technique based on Youngs' algorithm is used to investigate the effect of different parameters on the bubble growth characteristics. To validate the model, the results of simulations for the bubble shape during its growth from a cavity are compared with those of the experiments available in the literature. The effect of different parameters such as surface tension, viscosity, and injected gas flow rate on the bubble departure diameter is investigated.

1. INTRODUCTION

The bubble growth from a cavity on a solid surface and the diameter at which the bubble departs the surface (departure diameter) are important boiling characteristics discussed in many engineering applications. As an example, boiling mechanisms and boiling heat transfer play an important role in the performance of power generation equipments where the evaporation of a coolant is utilized to achieve high heat removal rate. Nucleate boiling is the major boiling mode in normal operation. In contrast, a transition to a film boiling would significantly decrease the heat transfer through low-conductivity vapor layer.

Most of the extensive research carried out on the generation of bubbles by injection of gas into a liquid at rest has been devoted to the important case of liquids of small viscosity. The flow is induced by the expansion, and the rise of the bubbles is dominated by inertial effects [1-4]. Applications include direct-contact operations in chemical, metallurgical, and biomedical systems, among many others. The opposite case of bubble generation in very viscous liquids is of interest in connection with polymer melts [5] and molten glasses and magmas [6, 7]; this case, however, has been comparatively less studied. Using a balance of buoyancy and viscous forces on the surface of each bubble, Davidson & Schuler [8] proposed that the volume of the bubbles injected in a very viscous quiescent liquid increases as the gas flow rate to power ¾, and is independent of the radius of the injection orifice. This estimate is intended to apply for high gas flow rates for which the effect of surface tension acting across the contact line of the attached bubble with the solid surface of the orifice is negligible. At very small flow rates, on the other hand, viscous forces are negligible during most of the growth of the bubble whose shape is determined by a hydrostatic balance of buoyancy and surface tension. In a recently presented model by Winterton [9], the bubble diameter is only a function of the column diameter. According to this model, the bubble size is independent of the orifice size and the physical properties of the liquid phase. It is, therefore, obvious that the effect of design parameters on bubble size is not well understood and that it deserves further investigation. The effects of liquid physical properties, such as surface tension, density and viscosity, have been studied by several investigators. While some researchers [10] have observed that the bubble size decreases with the addition of small amounts of organic compounds to the liquid phase, others [9] did not observe such a reduction.

Numerical studies of two-phase flows are carried out to analyze the interface behavior of one air bubble growing and rising in a viscous liquid. A well-known method for tracking the free surface of a liquid is Volume-of-Fluid (VOF) technique [12] where the computational domain is characterized by a scalar function whose value is one for a cell full of liquid and zero for an empty cell. A cell with a value between zero and one indicates a free-surface cell. Different methods based on VOF technique have been developed for advecting a liquid/gas interface; the most accurate one is believed to be that of Youngs [12] where the reconstruction of the interface is performed by piecewise linear segments cutting through computational cells. In this study, the bubble growth and departure from a cavity is modeled using this technique. The model is validated by a comparison of the numerical results with those of the experiments [11].

2. NUMERICAL METHOD

There are two main issues regarding the developed model: the advection of the cavity interface using VOF method, and the bubble growth model. In this section, we present these two parts.

2.1 VOF algorithm

The main issue regarding the developed model is the advection of the bubble interface using VOF method. In this section, we present a brief account of the numerical method. The flow governing equations are:

$$\vec{\nabla}\cdot\vec{V}=0 \tag{1}$$

$$\frac{\partial\vec{V}}{\partial t}+\vec{\nabla}\cdot(\vec{V}\vec{V})=-\frac{1}{\rho}\vec{\nabla}p+\frac{1}{\rho}\vec{\nabla}\cdot\vec{\tau}+\frac{1}{\rho}\vec{F}_b \tag{2}$$

where $\vec{V}$ is the velocity vector, p is the pressure and $\vec{F}_b$ represents body forces acting on the fluid. The bubble interface is advected using VOF method by means of a scalar field f whose value is unity in the liquid phase and zero in the gas. When a cell is partially filled with liquid, f will have a value between zero and one.

$$f=\begin{cases}1 & \text{in liquid}\\ >0,<1 & \text{at the liquid-gas interface}\\ 0 & \text{in gas}\end{cases} \tag{3}$$

The discontinuity in f is propagating through the computational domain according to:

$$\frac{df}{dt}=\frac{\partial f}{\partial t}+\vec{V}\cdot\vec{\nabla}f=0 \tag{4}$$

For the advection of volume fraction f based on Eq.4, different methods have been developed such as SLIC, Hirt-Nichols and Youngs' PLIC [12]. The reported literature on the simulation of free-surface flows reveals that Hirt-Nichols method has been used by many researchers. In this study, however, we used Youngs' method [12-14], which is a more accurate technique. Assuming the initial distribution of f to be given, velocity and pressure are calculated in each time step by the following procedure. The f advection begins by defining an intermediate value of f,

$$\tilde{f}=f^n-\delta t\vec{\nabla}\cdot(\vec{V}f^n) \tag{5}$$

Then it is completed with a "divergence correction"

$$f^{n+1}=\tilde{f}+\delta t(\vec{\nabla}\cdot\vec{V})f^n \tag{6}$$

A single set of equations is solved for both phases, therefore, density and viscosity of the mixture are calculated according to:

$$\begin{aligned}\rho&=f\rho_l+(1-f)\rho_g\\ \mu&=f\mu_l+(1-f)\mu_g\end{aligned}, \tag{7}$$

where subscripts l and g denote the liquid and gas, respectively. New velocity field is calculated according to the two-step time projection method as follows. First, an intermediate velocity is obtained,

$$\frac{\tilde{\vec{V}}-\vec{V}^n}{\delta t}=-\vec{\nabla}\cdot(\vec{V}\vec{V})^n+\frac{1}{\rho^n}\vec{\nabla}\cdot\vec{\tau}^n+\vec{g}^n+\frac{1}{\rho^n}\vec{F}_b^{\,n} \tag{8}$$

The continuum surface force (CSF) method [13, 14] is used to model surface tension as a body force ($\vec{F}_b$) that acts only on interfacial cells. A pressure Poisson equation is then solved to obtain the pressure field,

$$\vec{\nabla}\cdot[\frac{1}{\rho^n}\vec{\nabla}p^{n+1}]=\frac{\vec{\nabla}\cdot\tilde{\vec{V}}}{\delta t} \tag{9}$$

Next, new time velocities are calculated by considering the pressure field implicitly,

$$\frac{\vec{V}^{n+1}-\tilde{\vec{V}}}{\delta t}=-\frac{1}{\rho^n}\vec{\nabla}p^{n+1} \tag{10}$$

The cell size used in this study was set based on a mesh refinement study in which the grid size was progressively increased until no significant changes were observed in the simulation results. The mesh resolution was characterized by the number of cells per the bubble diameter. From the mesh refinement study, the optimum mesh size was found to be 15 cells per bubble radius. This mesh size was used for all simulations throughout this paper.

2.2 Bubble growth model

In a detailed study, Longuet-Higgins et al. [15] computed the equilibrium shapes of attached bubbles and the volume at which equilibrium ceases to be possible and the bubble should detach. In orders of magnitude, the volume of the bubble at detachment, V, is given in this small-flow-rate regime by the hydrostatic balance $\rho gV\sim\gamma a$, or $V/a^3\sim 1/B$ in dimensionless terms. ρ is the density of the liquid, γ the liquid–gas surface tension, a the radius of the injection orifice, and g the gravitational acceleration, and

$$B=\frac{\rho g a^2}{\gamma} \tag{11}$$

is the Bond number. If the growth of the bubble is due to the injection of a gas flow rate Q, then the velocity induced in the liquid by the expansion of the bubble is $v=O(Q/V^{2/3})$ and the viscous force of the liquid on the surface of the bubble is $F_v=O[(\mu v/V^{1/3})V^{2/3}]=O(\mu Q/V^{1/3})$, where μ is the viscosity of the liquid. This force is in the order of the buoyancy force ($F_v\sim\rho gV\sim\gamma a$) when $Q\sim\rho gV^{4/3}/\mu$ or, using the estimate of V above, when $Ca\sim 1/B^{1/3}$, where

$$\mathrm{Ca} = \frac{\mu Q}{\gamma a^2} \tag{12}$$

is the capillary number. At higher flow rates, the surface tension becomes negligible in the balance of forces on the bubble, which reduces to $Fv \sim \rho g V$, leading to (Davidson & Schuler [8])

$$\frac{V}{a^3} \sim \left(\frac{\mathrm{Ca}}{\mathrm{B}}\right)^{3/4} \tag{13}$$

The hydrostatic regime thus corresponds to $Ca << 1/B^{1/3}$, and the Davidson & Schuler [8] high-flow-rate regime should be attained for $Ca >> 1/B^{1/3}$. Wong et al. [16] numerically computed the time evolution of a single bubble from onset to detachment for a variety of Bond and capillary numbers, describing the transition between hydrostatic and high-flow-rate regimes. Zhang & Stone [17] extended this analysis to take into account the viscosity of the injected fluid. An additional complexity arises, however. The ratio of the growth time of a bubble ($t_{growth} \sim V/Q$) to the time it takes for a detached bubble to rise a distance of the order of its size ($t_{rise} \sim V^{1/3}/U$) is $t_{growth}/t_{rise} \sim (V^{4/3}/a^4)B/Ca$. The rise velocity U is estimated from the balance of buoyancy and viscous drag as $\rho g V \sim \mu U V^{1/3}$. The above time ratio is large in the hydrostatic regime but is in the order of unity in the transition regime and beyond leading to an interaction between successive bubbles and the possibility of coalescence in the vicinity of the injection orifice.

Tong et al. [18] explored the suitability of variety of bubble correlations for highly-wetting liquids including FC-72. They determined that the Cole and Rohsenow model [19] for the departure diameter best fits the available experimental data:

$$D_b = \sqrt{\frac{\sigma_w E}{g(\rho_l - \rho_g)}} \tag{14}$$

where

$$\mathrm{E} = (0.000465 \times Ja'^{5/4}) \tag{15}$$

and

$$Ja' = \frac{c_p \rho_l T_{sat}}{\rho_g h_{lg}} \tag{16}$$

with the saturation temperature is specified in absolute degrees. Tong et al. [18] modified the Cole and Rohsenow model [19] to include the wall temperature dependence of departure diameter by evaluating the surface tension in Eq. (14) at the wall temperature. Corresponding to a boiling surface superheat of 12.3°C, the mass flow rate for the vapor inlet, representing the nucleation site, may be calculated. The average vapor mass generation rate over the bubble growth time is

$$\dot{m} = \pi\left(\frac{D_b}{2}\right)^2 H \frac{\rho_g}{\tau_g} \tag{17}$$

As discussed in the following section, the vapor inlet representing the nucleation site in the CFD model is taken to be 1 mm in size. Combining this value with Eq. (17) yields an expression for the average vapor mass flux over the bubble growth time as:

$$G = \pi\left(\frac{D_b}{2}\right)^2 \frac{\rho_g}{s\tau_g} \tag{18}$$

where s is the size of the vapor inlet, and the channel depth factor is out of the problem.

In the simulation, the bubble growth from the cavity is modeled by the injection of a gas flow at the fluid/cavity interface. This technique was employed in experiments performed by Fritz [20] using which he proposed a correlation for the bubble departure diameter as a function of the injected gas flow rate. The bubble departure diameter was determined by a balance between the buoyancy and surface tension forces acting normal to the solid surface. Staniszewski [21] modified the Fritz correlation based on his experimental measurement of the departure diameter over a range of pressure and on observation of the influence of the bubble growth rate on the departure diameter. His correlation reads:

$$D_d = 0.0071 \times \beta\left(\frac{2\gamma}{g\Delta\rho}\right)^{1/2}\left(1 + 34.3\frac{\partial D}{\partial t}\right) \tag{19}$$

where $\partial D/\partial t$ is the bubble growth rate which increases with the gas flow rate Q, β is the static contact angle, γ the surface tension and $\Delta\rho$ the difference between the liquid and vapor densities.

3. RESULTS AND DISCUSSION

The first case considered for simulation of the bubble growth deformation from a cavity was that of an experiment performed by Brian et al. [11] in which the cavity diameter was 2.08 mm. The experimental photographs along with numerical predictions for this case are shown in Fig. 1. The time interval between sequential images is 1/30 s for both photographs and numerical images. The figure shows that as the bubble grows from the cavity its shape is changing from a sphere to an elongated oval due to the buoyancy effects. With further growth of the bubble, both model and experiment predict the formation of a neck in the bubble shape. Soon after the neck appears, the bubble center accelerates upward and it departs. To compare the two results quantitatively, the dimensionless height of the bubble (the height divided by the cavity diameter) from the experiment [11] and numerical model is shown in Fig. 2. A good agreement between the two results validates the model and its underlying assumptions.

The results of the numerical model are also compared with the measurements of a separate experiment performed by Qiu et al. [22]. Figure 3

shows a quantitative comparison of the model predictions and measurements [22] for the growth history of the equivalent bubble diameter. The equivalent diameter is the diameter of a sphere having the same volume as the bubble. As seen from the figure, numerical predictions well agree with those of the measurements.

Next, we studied the effects of important parameters on the bubble growth phenomenon. These parameters include surface tension, viscosity and injected gas flow rate. The default material properties used in the simulations are given in Table 1.

properties	water	air
density	ρ_l=998.2 kg/m^3	ρ_a=1.1222 kg/m^3
viscosity	μ_l=1002×10^{-6} kg/(m.s)	μ_a=18.24×10^{-6}kg/(m.s)
surface tension	γ=0.073 N/m	

Table 1: Material properties.

There are contradicting reports about the effect of cavity size on mean bubble diameter. Several researchers reported that the bubble diameter is independent of the cavity size [23] while others [24] showed that the cavity diameter has a strong effect on the bubble diameter leaving the cavity plate. The most common types of gas distributor used in bubble column reactors are perforated plates where cavity diameters from 0.5 to 3 mm are placed in the corners of equilateral triangles at distances between centers (pitch) of about 15 to 20 mm [25].

The effect of cavity diameter on the mean bubble diameter from the model and experiments [26] is presented in Fig. 4. The results show that the bubble departure diameter increases as the cavity diameter is increased from 2 to 3 mm. The surface tension and viscous forces are two major contributing forces influencing the bubble diameter during its formation. At very small flow rates, the bubble diameter is controlled entirely by surface tension and buoyancy forces. At high gas flow rates, in the case of liquids with low viscosity, the effect of surface tension is generally considered negligible. To verify the effect of surface tension, numerical studies are performed for solutions of propanol concentrations, and hence different surface tension values, at low, medium and high flow rates. The results are presented in Fig. 5. These predicted results are also compared with experimental data [26] which were systematically collected for different liquid mixtures. A good agreement is observed between simulations and experiments. It should be mentioned that although the effect of surface tension is considerably reduced as the flow rate is increased, this effect cannot be completely ignored even at high flow rates. The results also indicate that the VOF method predicts the well-known relation $D \sim \gamma^{1/2}$ (from Eq. 19).

Figure 6 displays the effect of liquid viscosity on bubble size predicted from the simulation and measured from experiments [26] for a range of liquid mixtures with glycerol. A close agreement is seen between the predicted data and those of the experiments. While the influence of the viscosity is negligible at low gas flow rates, it becomes important at high gas flow rates where an increase in viscosity increases the bubble size.

The effect of gas flow rate on the bubble volume is presented in Fig. 7. As expected, increasing the gas flow rate increases the bubble volume. The model predictions are also compared with experimental data [27] where a good agreement is observed between the two results.

Finally, the numerical results are compared with visualizations of bubble formation and coalescence in a silicone oil with properties of μ=*9.68* Pa.s (at 25◦C), ρ =968Kgm^{-3} and γ =2.15×10−2Nm^{-1}. Air was injected through an orifice with an internal diameter of 0.25 to 0.5mm sticking out of the centre of the base of a vertical cylindrical container of 8.6 cm in diameter filled with oil to a height of 20 cm above the tip of the needle. At *Ca=7* the coalescence of the two bubbles occurs at about the same time as the detachment of the leading bubble of the following couple. When the capillary number increases above *Ca≈15*, the coalescence occurs before the trailing bubble of each couple has had time to detach from the orifice. Figure 8 shows the coalescence phenomenon for a separated bubble and a bubble still attached to the injection cavity. A good qualitative agreement is seen between the photographs [28] and calculated images in the same instances of the process. The same conditions as of the experiments were applied in the simulation.

4. CONCLUSIONS

In this paper, an axisymmetric VOF method was used to simulate the bubble growth and departure of a bubble from a cavity. The model was validated by a comparison between numerical results for the bubble shape during its growth from a cavity with those of the experiments available in the literature. Next, we studied the effects of important parameters on the bubble growth phenomenon. These parameters included surface tension, viscosity, and injected gas flow rate. Increasing surface tension and/or viscosity increased the bubble departure diameter. The surface tension was observed to be an important factor contributing to the bubble volume and, therefore, it should be taken into consideration even at high gas flow rates. The bubble size is also strongly dependent on the cavity diameter over a wide range of gas flow rates. Finally we studied the coalescence of sequential bubbles detached from a cavity, and compared the images with those of the experiments [28]. The numerical results were in good qualitative agreement with photographs.

REFERENCES

[1] Kumar, R. & Kuloor, N. R., The formation of bubbles and drops, *Adv. Chem. Engineering*, 8, 255–368, 1970

[2] Clift, R., Grace, J. R. and Weber, M. E., Bubbles, Drops, and Particles. Academic, 1978.

[3] Rabiger, N. and Vogelpohl, A., Bubble formation and its movement in newtonian and non-newtonian liquids. *In Encyclopedia of Fluid Mechanics*, 3, Chapter 4 (ed. N. P. Cheremisinoff), Gulf. 1986.

[4] Sadhal, S. S., Ayyaswamy, P. S. and Chung, J. N., Transport Phenomena with Drops and Bubbles, Chapter 7, *Springer*, 1997.

[5] Bird, R. B., Armstrong, R. C. and Hassager, U., Dynamics of Polymeric Liquids, John Wiley, 1987.

[6] Sahagian, D. L., Bubble migration and coalescence during solidification of basaltic lava flows, *J. Geol*. 93, 205–211, 1985.

[7] Manga, M. and Stone, H. A. Interactions between bubbles in magmas and lavas: Effects of the deformation, *J. Volcano*, Res. 63, 269–281, 1994.

[8] Davidson, J. F. and Schuler, B. O. G., Bubble formation at an orifice in a viscous liquid. *Trans. Inst. Chem. Engrs*, 38, 144–154, 1960.

[9] Winterton, R. H. S., A simple method of predicting bubble size in bubble columns, *Chem Eng Proc*, 33, 1–5., 1994

[10] Zieminski, S. A., Caron, M. M. and Blackmore, R. B., Behavior of air bubbles in dilute aqueous solutions, *Ind Eng Chem Fund*, 6, 233–242, 1967.

[11] Brian K., Mori, W. and Baines D., Bubble departure from cavities, *Int. J. Heat Mass Transfer*. 44: 771-783, 2001.

[12] Hirt, C.W. and Nichols, B.D., Volume of fluid (VOF) method for the dynamics of free boundaries. *J Comput Phys*, 39: 201, 1981.

[13] Bussmann M., Mosthghimi J., and Chandra S., On a Three-Dimensional Volume Tracking Model of Droplet Impact, *Phys. Fluid*, 11: 1406, 1999.

[14] Passandideh-Fard, M., and Roohi, E., Transient Simulations of Cavitating Flows using a Modified Volume-of-Fluid (VOF) Technique, *Int. J. of Comput. Fluid Dynamics*, 22, 97-114, 2008.

[15] Longuet-Higgins, M. S., Kerman, B. R. and Lunde, K. The release of air bubbles from an underwater nozzle. *J. Fluid Mech*. 230, 365–390, 1991.

[16] Wong, H., Rumschitzki, D. and Maldarelli, C., Theory and experiment on the low-Reynolds number expansion and contraction of a bubble pinned at a submerged tube tip. *J. Fluid Mech*. 356, 93–124, 1998.

[17] Zhang, D. F. and Stone, H. A. Drop formation in viscous flows at a vertical capillary tube. *Phys. Fluids* 9, 2234–2242, 1997.

[18] Tong, W., Bar-Cohen, A., and Simon, T.W., Thermal transport mechanisms in nucleate pool boiling of highly-wetting liquids, *Proceedings of the Ninth International Heat Transfer Conference*, 2, 27–32, 1990.

[19] Cole, R. and Rohsenow, W.M., Correlation of bubble departure diameters for boiling of saturated liquids, *AIChE Chemical Engineering Progress Symposium Series*, 65, 211–213, 1969.

[20] Fritz W., Maximum volume of vapor bubbles, Physik Zeitschr, 36, 379–384, 1935.

[21] Staniszewski B.E., Nucleate boiling bubble growth and departure, *MIT Tech*. Rep. No. 16, Cambridge, MA, 1959.

[22] Qiu, D.M., Dhir, V.K., Hasan, M.M. and Chao, D., Single Bubble Dynamics during Nucleate Boiling under Low Gravity Conditions, *Microgravity Fluid Physics and Heat Transfer*, Editor: V.K. Dhir, Begell house, New York : 62-71, 2000.

[23] Akita, K. and Yoshida, F., Bubble size, interfacial area and liquid phase mass transfer coefficient in bubble columns, *Ind Eng Chem Process Des Dev*, 13: 84–91, 1974.

[24] Kumar, A., Degaleesan, T. E., Laddha, G. S. and Hoelscher, H. E., Bubble swarm characteristics, *Can J Chem Eng*, 54: 503–509, 1976.

[25] Smith, E. L., Jamialahmadi, M., Olajuyigbe, J. T. and Shayegan-Salek, J., The effect of operating conditions on gas holdup and mixing in bubble columns, *Int Conf On Bioreactor Fluid Mechanics, Cambridge,* UK: 45–59, 1986.

[26] Jamialahmadi, M., Zehtabian, M. R., Muller-steinhagen, H., Saraffi A., and Smith, J. M., Study of bubble formation under constant flow conditions, *Trans IChemE*, 79, Part A, 2001.

[27] Tsuge, H. Terasaka, K. Koshidat, H. and Matsue, H., Bubble formation at submerged nozzles for small gas flow rate under low gravity, *Chemical Eng. Sci*., 52, No. 20: 3415-3420, 1997.

[28] Higuera, F. J., Injection and coalescence of bubbles in a very viscous liquid, *J. Fluid Mech*, 530 :369–378, 2005.

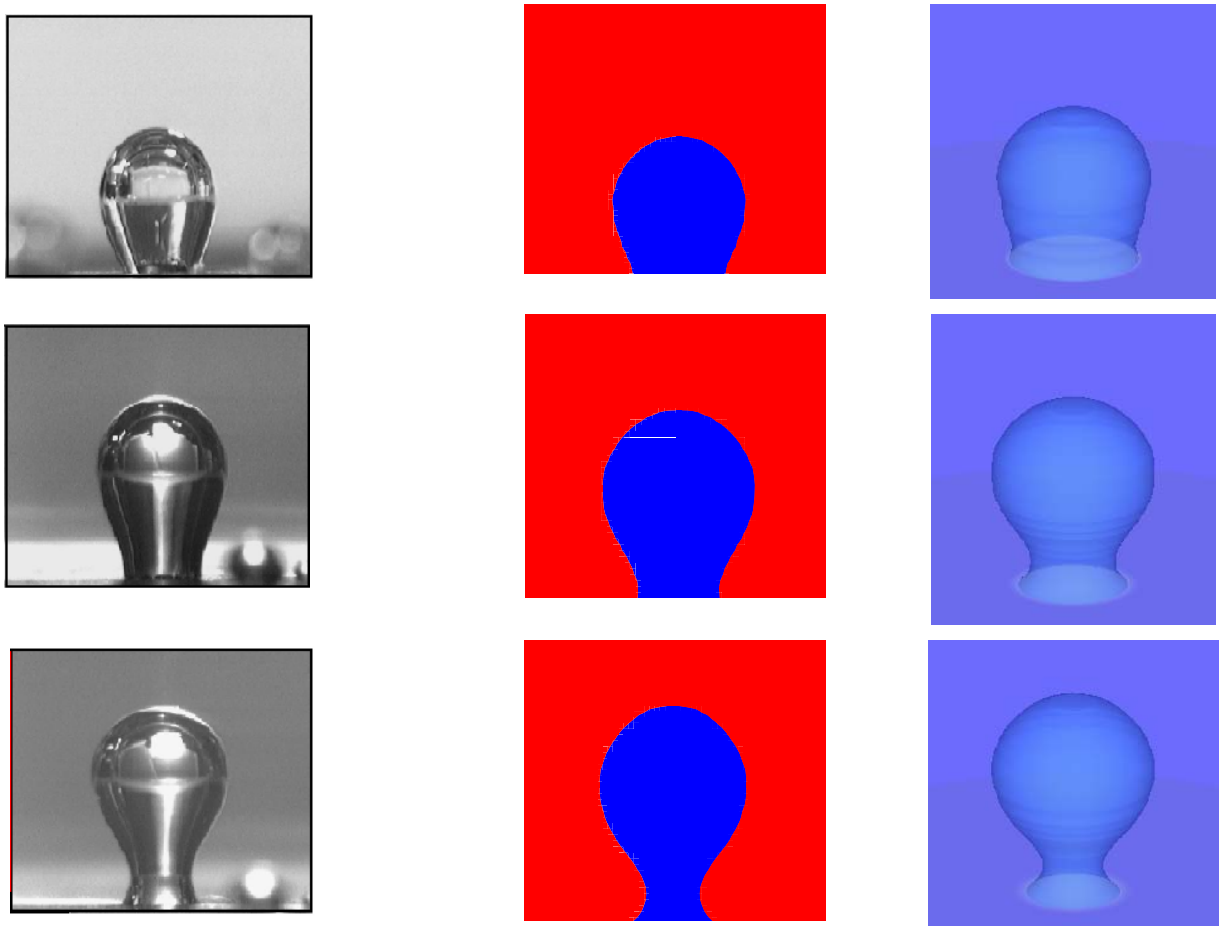

Figure 1. Comparison of bubble shapes from experiments [11] and numerical model (both cross-sectional area and 3D views) for a cavity with a diameter of d=2.08 mm. Images of bubble departure are taken 1/30 s apart.

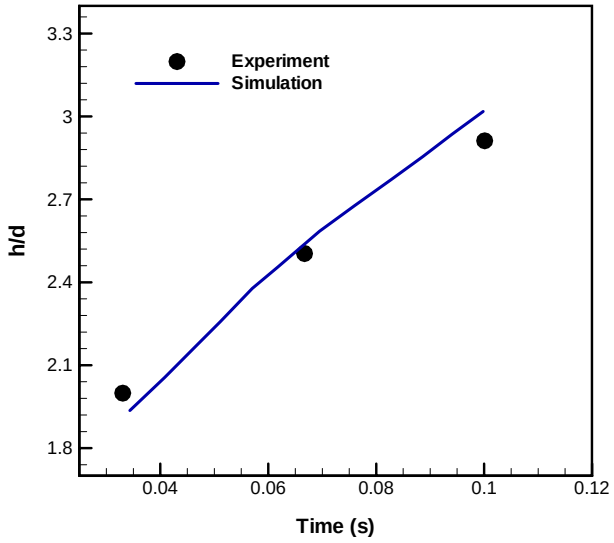

Figure 2. Time variation of dimensionless bubble height from simulations and experiments [11] for a cavity with a diameter of d=2.08 mm.

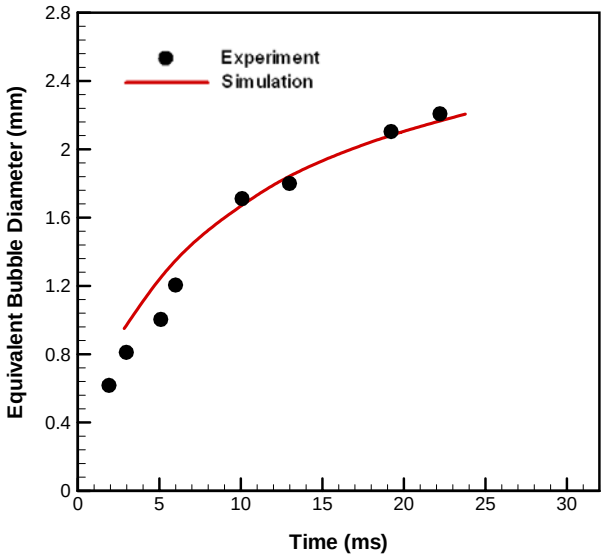

Figure 3. The evolution of bubble growth against time from simulations and experiments [22].

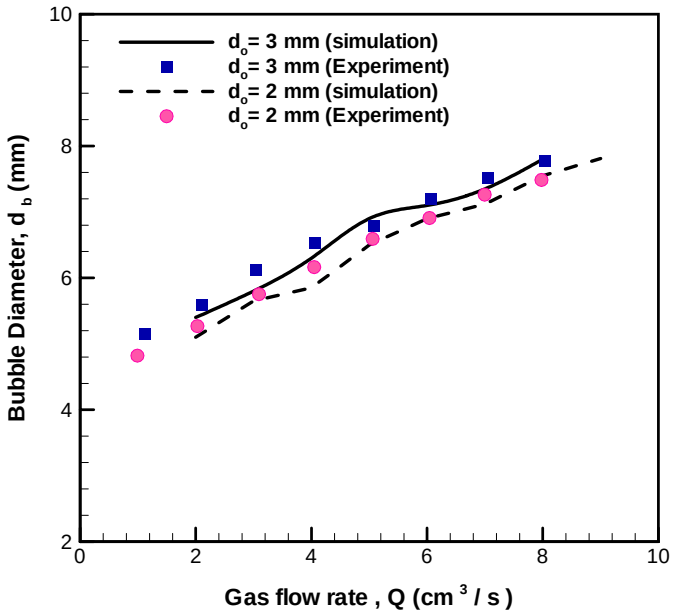

Figure 4. Bubble departure diameter against injected gas flow rate at different cavity diameters from simulations and experiments [26].

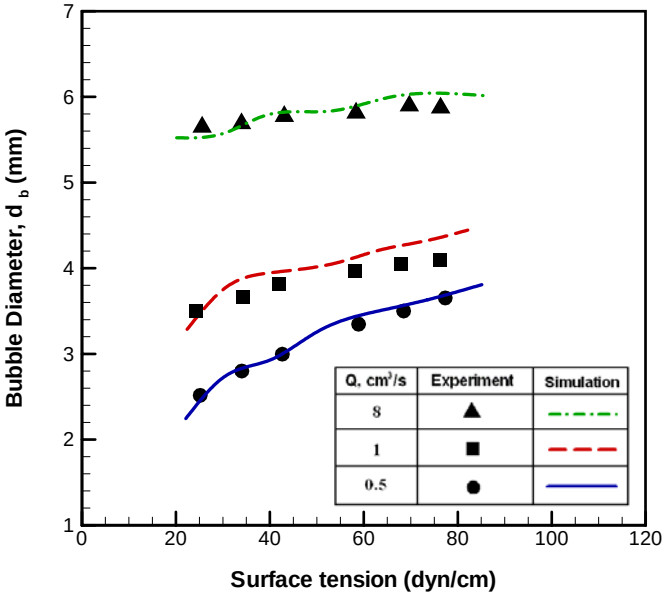

Figure 5. Effect of surface tension on bubble departure diameter at different gas flow rates for a cavity with d=2 mm from simulations and experiments [26].

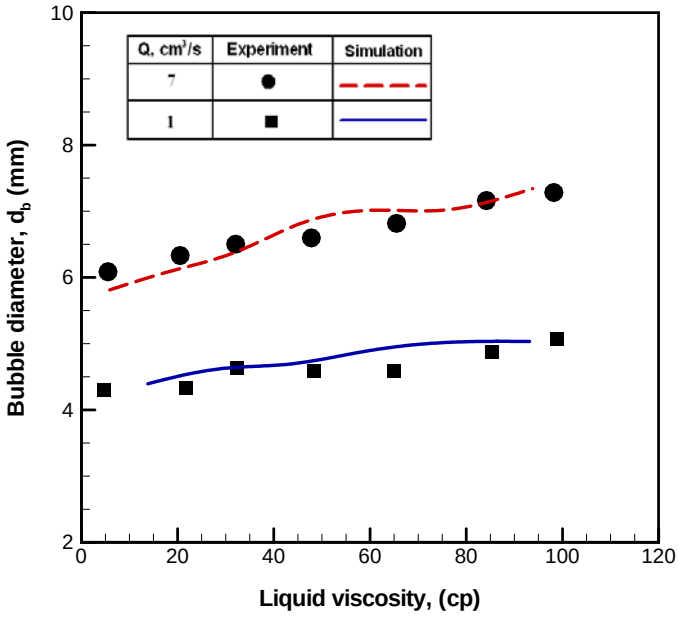

Figure 6. Effect of liquid viscosity on bubble departure diameter at different gas flow rates for a cavity with d=2 mm from simulations and experiments [26].

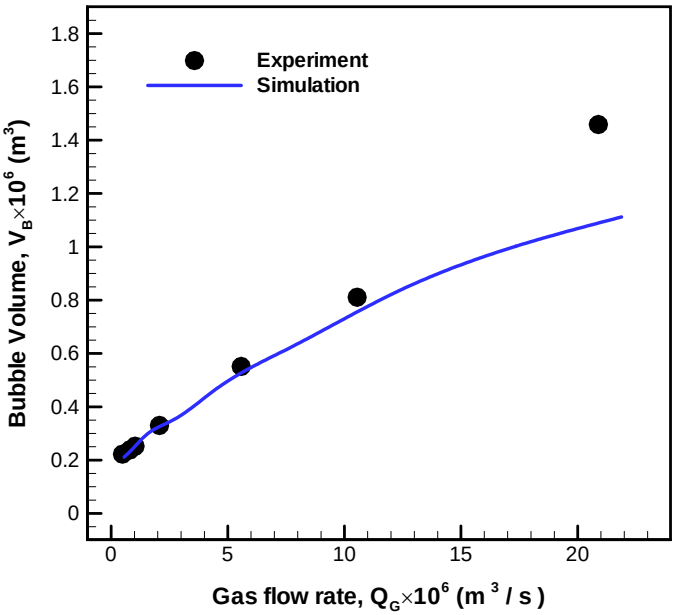

Figure 7. Effect of gas flow rate on bubble volume from simulations and experiments [27].

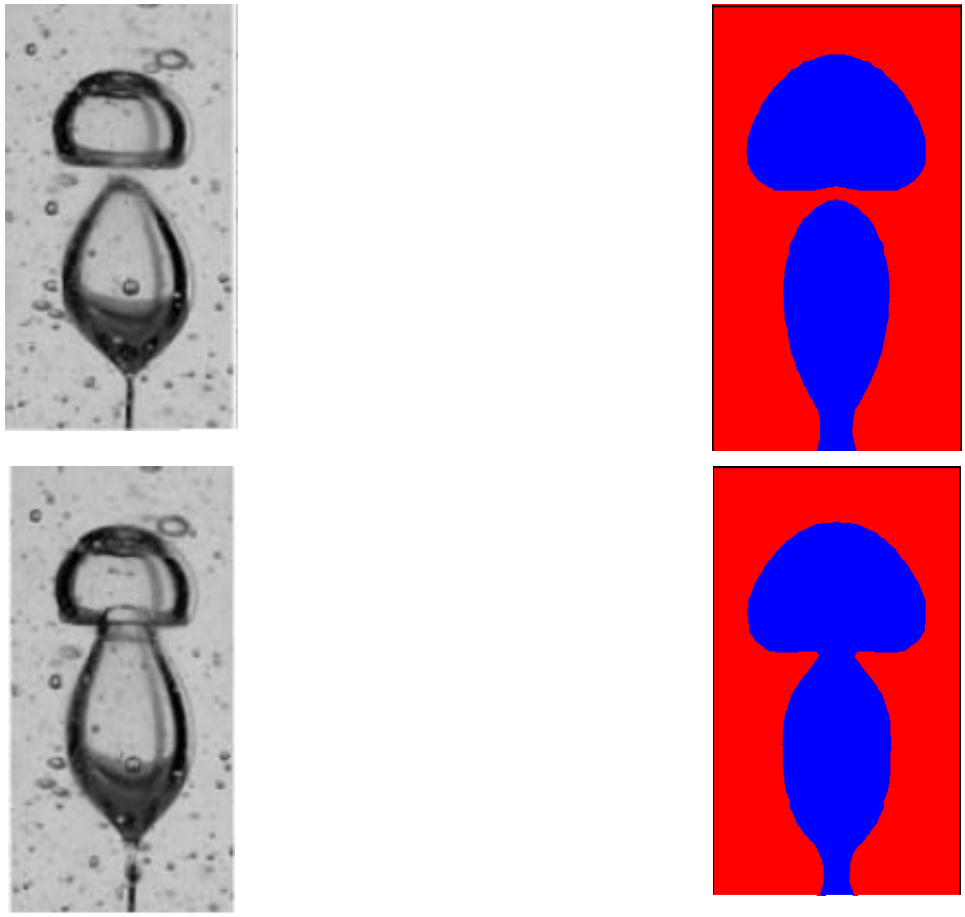

Figure 8. The coalescence of two sequential detached bubbles from experiments [28] and numerical model for a cavity with a diameter of d=0.5 mm and a gas flow rate of Q=1.3 cm^3/s (Ca=*950*).